

Formation of SXT Tandem Arrays and SXT-R391 Hybrids

Vincent Burrus and Matthew K. Waldor*

Department of Molecular Biology and Microbiology, Tufts University School of Medicine, and
Howard Hughes Medical Institute, Boston, Massachusetts 02111

Received 19 November 2003/Accepted 23 January 2004

SXT is an integrative and conjugative element (ICE) isolated from *Vibrio cholerae*. This ~100-kb ICE encodes resistance to multiple antibiotics and integrates site specifically into the chromosome. SXT excises from the chromosome to form a circular but nonreplicative extrachromosomal molecule that is required for its transfer. Here we found that a significant fraction of freshly isolated SXT exconjugants contained tandem SXT arrays. There was heterogeneity in the size of the SXT arrays detected in single exconjugant colonies. Some arrays consisted of more than five SXTs arranged in tandem. These extended arrays were unstable and did not persist during serial passages. The mechanism accounting for the generation of SXT arrays is unknown; however, array formation was not dependent upon *recA* and appeared to depend on conjugative transfer. While such arrays did not alter the transfer frequency of wild-type SXT, they partially complemented the transfer deficiency of a Δ *xis* SXT mutant, which is ordinarily unable to generate the extrachromosomal intermediate required for SXT transfer. Exconjugants derived from donor strains that harbored tandem arrays of SXT and R391, an SXT-related element, contained functional hybrid elements that arose from *recA*-independent recombination between the two ICEs. Thus, arrays of SXT-related elements promote the creation of novel ICEs.

The integrative and conjugative elements (termed ICEs) are a diverse class of mobile elements that share a similar lifestyle in both gram-positive and gram-negative bacteria (5, 26). Like most prophages, ICEs are maintained integrated within the chromosome of their hosts. They excise from the chromosome by recombination between two specific flanking sequences (*attL* and *attR*) to form a covalently closed circular molecule that is generally not replicative. Like the conjugative plasmids, ICEs encode conjugation systems that can transfer the excised DNA to a new host, where it integrates once again, often in a site-specific fashion, by recombination between the *attP* site generated by excision and a target sequence, *attB*. Different ICEs integrate into a variety of sites and encode diverse recombination, conjugation, and regulation systems (5). They also carry genes encoding a variety of functions, including catabolic pathways (26), antibiotic resistances (21, 29), nitrogen fixation (24), and phage resistance mechanisms (6).

The 99.5-kb SXT element (SXT) is a *Vibrio cholerae*-derived ICE that was originally identified in a 1993 *V. cholerae* serogroup O139 clinical isolate, MO10 (28). The MO10-derived SXT, SXT^{MO10}, encodes resistance to sulfamethoxazole, trimethoprim, chloramphenicol, and streptomycin, and its complete nucleotide sequence has been determined (2). SXT^{MO10}-related elements are now present in most (if not all) *V. cholerae* O139 and *V. cholerae* O1 clinical isolates from Asia (15). Some of these SXT-related elements contain different antibiotic resistance genes or even lack antibiotic resistance genes. Recently, SXT-related elements were detected in *V. cholerae* O1 clinical isolates from Africa (10) and in non-O1 and non-O139 clinical isolates from India (25). Furthermore, SXT has also been found in *Providencia alcalifaciens* clinical isolates from

Bangladesh, indicating that SXT elements are not unique to *V. cholerae* (15). In the laboratory, SXT transfers by conjugation to a variety of gram-negative bacteria, including *V. cholerae* and *Escherichia coli*.

SXT encodes a tyrosine recombinase (Int) that catalyzes its integration into the 5' end of *prfC*, a gene encoding peptide chain release factor 3 (17). SXT excision from the chromosome also requires Int and is greatly facilitated by a recently described Xis protein (7). Deletion of either *int* or *xis* from SXT nearly eliminates SXT transfer, suggesting that the circular extrachromosomal form of SXT is a required intermediate in its transfer (7). Both SXT integration and excision are under the control of SXT-encoded transcriptional activators, SetC and SetD, which also activate the expression of the transfer functions (2, 7). SetC and SetD expression is repressed by a lambda CI-like repressor, SetR. SetR-mediated repression was recently found to be alleviated by the SOS response to DNA damage in a RecA-dependent fashion (3).

R391 is an ICE originally isolated in 1972 in South Africa from *Providencia rettgeri* that mediates resistance to kanamycin and mercury (9). R391 and several related IncJ elements integrate into *prfC*, the same chromosomal locus used by SXT. In fact, SXT and R391 are genetically and functionally related (14). Comparison of the nucleotide sequences of these two ICEs showed that they consist of a conserved set of genes that mediate regulation, excision/integration, and conjugative transfer of the respective ICEs (1). Insertions into this shared common backbone confer element-specific properties such as resistance to particular antibiotics. SXT and R391 do not exclude each other, and in cells harboring both elements, SXT and R391 are found integrated in tandem fashion on the chromosome (14). In cells that harbor tandem SXT-R391 arrays, each element can excise and transfer independently of the other.

In the present study, we found that SXT transfer into *E. coli* and *V. cholerae* recipients often resulted in the formation of

* Corresponding author. Mailing address: Department of Molecular Biology and Microbiology, Tufts University School of Medicine, Jaharis 425, 136 Harrison Ave., Boston, MA 02111. Phone: (617) 636-2730. Fax: (617) 636-2723. E-mail: matthew.waldor@tufts.edu.

TABLE 1. Bacterial strains and plasmids used in this study

| Strain or plasmid | Genotype or phenotype | Reference or source |
|--------------------|---|----------------------------------|
| <i>E. coli</i> | | |
| CAG18439 | MG1655 <i>lacZU118 lacI42::Tn10</i> | 23 |
| KB1 | MG1655 <i>recA56 gutA52 gutR::Tn10</i> | K. Bettenbrock, unpublished data |
| HW220 | CAG18439 <i>prfC::SXT</i> | 17 |
| BI533 | MG1655 <i>Nal^r</i> | 16 |
| BW25113 | <i>lacI^q rrnB₁₄ ΔlacZ_{WJ16} hsdR514 ΔaraBAD_{AH33} ΔrhaBAAD_{LD78}</i> | 11 |
| JO115 | CAG18439 <i>prfC::R391-SXT</i> | 14 |
| JO116 | CAG18439 <i>prfC::SXT-R391</i> | 14 |
| MW5-39 | MC4100 <i>srI::Tn10 F⁻ araR131 Δlac(U169) rpsL thiA recA1</i> | 18 |
| VI31 | CAG18439 <i>ΔprfC</i> | This study |
| VI47 | KB1 <i>ΔprfC</i> | This study |
| VI166 | BW25113 <i>prfC::SXT</i> | This study |
| VI200 | MG1655 <i>prfC::SXT Δxis pXis</i> | This study |
| VI227 | KB1 <i>prfC::R391 Δxis-SXT Δxis pSetCD</i> | This study |
| VI228 | KB1 <i>prfC::SXT Δxis-R391 Δxis pSetCD</i> | This study |
| <i>V. cholerae</i> | | |
| MO10 | Toxigenic 1992 serogroup O139 clinical isolate from India, SXT ^{MO10+} | 27 |
| E4 | E1 Tor strain, <i>ΔctxABN4 Km^r</i> | 12 |
| Plasmids | | |
| pVI8A | pCRII-Topo <i>attP</i> | 7 |
| pSetCD | pBAD-Topo <i>setCD</i> | 2 |
| pXis | pBAD-Topo <i>xis</i> | 7 |

extended tandem SXT arrays. These arrays had variable numbers of constituent SXTs and were sometimes greater than 500 kb in size. Donor strains harboring both SXT and R391 yielded hybrid ICEs in exconjugant cells. Conjugative transfer from donors containing SXT and R391 appeared to be required for formation of hybrid ICEs, but homologous recombination appeared to play no role in their generation. Our findings suggest that tandem ICE arrays may be a source of ICE diversity, creating novel genetic combinations from preexisting elements.

MATERIALS AND METHODS

Bacterial strains, plasmids, and media. The bacterial strains and plasmids used in this study are described in Table 1. The *ΔprfC* mutants *E. coli* VI31 and VI47 were created as previously described (7). Bacterial strains were routinely grown in Luria-Bertani (LB) broth at 37°C on a roller drum incubator and were maintained at –80°C in LB broth containing 15% (vol/vol) glycerol. Antibiotics were used at the following concentrations: ampicillin, 100 μg/ml; chloramphenicol, 20 μg/ml; kanamycin, 50 μg/ml; nalidixic acid, 40 μg/ml; streptomycin, 200 μg/ml; sulfamethoxazole and trimethoprim (SXT), 160 and 32 μg/ml, respectively; tetracycline, 12 μg/ml.

Bacterial conjugations. Conjugation assays were performed by mixing equal volumes of overnight cultures of donor and recipient strains. The cells were harvested by centrifugation and resuspended in a 1/20 volume of LB broth. The cell suspensions were poured onto LB plates, supplemented when necessary with 0.02% arabinose or 0.2% glucose. The conjugation experiments were performed at 37°C for 6 h. Afterwards, the cells were harvested from the plate in 1 ml of LB medium, and serial dilutions of the cell suspensions were plated on the appropriate selective media to determine the numbers of donors, recipients, and exconjugants.

Molecular biology techniques. Plasmid DNA was prepared with either a Qia-prep Spin miniprep kit or a Qia-prep miniprep kit (Qiagen), and chromosomal DNA was prepared with the G Nome DNA kit (Q-Biogene) as described in the manufacturer's instructions. Southern blotting was performed as described previously (27) with probes conjugated to horseradish peroxidase and detected with a chemiluminescent substrate (Amersham). The *attP* probe was the 600-bp BstBI fragment of pVI8A (7). The PCR assays to characterize the structure of SXT, R391, or the hybrid elements were performed with the primers described in Table 2 in 20-μl PCR mixtures with a HotStarTaq master mix kit (Qiagen) by using 1 μl of a mixture of a colony resuspended in 8 μl of LB broth as a template.

The PCR conditions were as follows: (i) 15 min at 95°C; (ii) 30 cycles of 20 s at 95°C, 30 s at 50°C, and 30 s at 72°C; and (iii) 2 min at 72°C. *E. coli* chromosomal DNA used for contour-clamped homogenous electric field gel electrophoresis (8) was prepared by following the method of Heath et al. (13). After digestion by restriction enzymes, large *E. coli* restriction fragments were separated in a 1% agarose gel (Invitrogen) for 30 h by using a CHEF-DR II system (Bio-Rad) with the following settings: initial time, 1 s; final time, 40 s; voltage, 5 V/cm. Electrophoresis buffer was 0.5× Tris-borate-EDTA, which was maintained at 14°C during electrophoresis. Real-time quantitative PCR experiments were carried out as previously described (7) to measure the percentages of cells in a culture that contained unoccupied *attB* sites (EattBF and EattBR primers) and the SXT or R391 *attP* sequence (SXTJF and SXTJR primers). The amounts of both *attB* and *attP* were normalized to the amount of chromosomal DNA in each sample and expressed as the number of sites per 100 chromosomes.

RESULTS

Transfer of SXT promotes transitory formation of SXT tandem arrays in recipients. We recently developed quantitative PCR assays to measure the amounts of SXT *attB* and *attP* sequences in cell cultures (7). We expected that the amount of *attB* would reflect the number of unoccupied SXT integration sites, that the amount of *attP* would reflect the number of excised circularized SXT molecules, and that these numbers would be approximately equal. Surprisingly, we found that for exconjugants derived from a single mating, the percentages of *attB* and *attP* were not comparable. While the percentages of *attB* hardly differed between exconjugants, the percentages of *attP* were highly variable. For example, VI179 and VI180, two exconjugants derived from the same mating, had *attP* percentages of 8.3 and 114.8, respectively; the *attB* percentages were 1.7 and 2.9, respectively (Table 3).

The pronounced variation in the amounts of SXT *attP* sequences present in freshly derived exconjugants from the same or independent matings was also evident in Southern blots (Fig. 1A). The chromosomal DNAs of 10 exconjugants derived from five independent matings were probed with an SXT *attP*

TABLE 2. DNA sequences of oligonucleotides used in this study

| Primer | Gene or sequence specified | Nucleotide sequence (5'-3') |
|---------|-----------------------------------|-----------------------------|
| VISLF | SXT and R391 <i>attL</i> sequence | GAGTACAAATTCCGTTTTAG |
| VISLR3 | SXT <i>attL</i> sequence | GCATTCTCCTGAAAATCAATG |
| VISRF | SXT and R391 <i>setR</i> gene | CTCTCATTAACCTGGGTTTCAGG |
| VISRR | SXT <i>attR</i> sequence | AATGGTTATCTGATCTGTTACCA |
| VISLR2 | R391 <i>orf1</i> gene | CGCATCAAACTCCCTAAG |
| VISRR2 | R391 <i>attR</i> sequence | AATGGTTATCTAATCGGCTATCA |
| MER104A | R391 <i>mer</i> gene | GCCTGAACGCTTTAGCT |
| MER103B | R391 <i>mer</i> gene | CTGCTCGGTTCCATCAT |
| 10SF13 | SXT <i>s037</i> gene | TTGTGGTGGAAGAGGGTG |
| SXT1-13 | SXT <i>s037</i> gene | CCAACAAAGAACAGTTTGACTC |
| ORF16 | SXT <i>s052</i> gene | CATCTACCACTTCATAGGCAGC |
| YND2 | SXT <i>s052</i> gene | CAGCTTAACTCACCAGGAC |
| EattBF | <i>attB</i> sequence | GCCGCACCTTTGCCATTATT |
| EattBR | <i>attB</i> sequence | AGCAGCACCTTCTCGGTGAT |
| SXTJF | SXT and R391 <i>attP</i> sequence | GCGAAGGACCTTTGCTATCATC |
| SXTJR | SXT and R391 <i>attP</i> sequence | TGGTTTTAAGCGTTGAAAGGC |

fragment. Five of ten of the exconjugants studied had a high copy number of a 4-kb SXT *attP*-specific fragment (Fig. 1A). Furthermore, the intensity of this fragment varied in these five exconjugants and did not correlate with the intensity of the *attL*- and *attR*-containing fragments, which remained constant (Fig. 1A).

The amplified 4-kb *attP* fragment could be derived from circular extrachromosomal SXT or from tandemly arranged chromosomally integrated SXTs. The former possibility seemed unlikely, as we were unable to extract a circular form of SXT from strains with amplified *attP* with several alkaline lysis-based techniques (22). Therefore, we used pulsed-field gel electrophoresis to assess whether the amplified *attP* sequence represented integrated copies of SXT arranged in tandem. For these analyses, DNA from CAG18439, which does not contain SXT, HW220, which contains a single SXT, and VI186, an exconjugant which contains amplified *attP* (Fig. 1A), were digested with *Sal*I or *Spe*I, two enzymes which do not cut in SXT. The fragments were separated by contour-clamped homogeneous electric field gel electrophoresis (PFGE) (Fig. 1B). Compared to the *Sal*I and *Spe*I restriction patterns of CAG18439, a single new band was observed in the *Sal*I- and *Spe*I-digested DNA from HW220, which contains a single SXT. In contrast,

five new bands appeared in both the *Sal*I- and *Spe*I-digested DNA of VI186. The first band from the *Sal*I-digested DNA (Fig. 1B, band 1) had a size identical to the band containing a single SXT integrated into *prfC*, as seen in HW220 DNA, but was less intense. Bands 2, 3, and 4 had sizes consistent with the presence of two, three, and four SXTs integrated in a tandem fashion into *prfC*. The band corresponding to the tandem array of three SXTs (band 3) had the strongest intensity in both restriction patterns, suggesting that this was the most prevalent arrangement in the cell population tested. The new band of highest molecular weight (5+) migrated out of the range of resolution of the gel and contained a tandem array of five or more SXTs. Bands 1 to 5+ all hybridized with an *attP* probe (data not shown), confirming that they contained SXT DNA. A similar distribution of bands was observed with *Spe*I-digested VI186 DNA; however, these bands differed in their molecular weights, confirming that the arrays were located on the chromosome. Thus, VI186, a population resulting from a single exconjugant, contains different-sized tandem arrays of SXTs. These findings illustrate the remarkable heterogeneity in the population of SXT exconjugants.

We wondered whether tandem SXT arrays formed in SXT's natural host, *V. cholerae*, as well as in *E. coli*. Southern blot analysis of exconjugants resulting from a mating between the *V. cholerae* clinical isolate MO10 (27), used as a donor, and *V. cholerae* E4 (12), used as a recipient, revealed that 2 of 10 exconjugants harbored tandem SXT arrays (Fig. 1C). This result indicates that tandem SXT arrays form in *V. cholerae* as well as in *E. coli* and that *E. coli* is a suitable SXT host to study this phenomenon.

To investigate the stability of SXT tandem arrays in *E. coli*, VI186 was cultivated for 5 days with two daily dilutions into fresh LB liquid medium (>200 generations) without selection for the SXT markers. After this time, DNA was isolated from this culture (now called VI218) and the copy number of SXT was analyzed by PFGE as described above. In VI218, the mean copy number of SXT appeared to be one, since only a single band (like that in HW220) was detected (Fig. 1B). This indicates that the high SXT copy number present in VI186 decreased under nonselective conditions. On the other hand, single integrated SXTs were not found to amplify even in the

TABLE 3. Quantification of unoccupied *attB* and *attP* sites by real-time quantitative PCR^a

| Exconjugant | % <i>attB</i> | % <i>attP</i> | Ratio ^b |
|-------------|---------------|---------------|--------------------|
| HW220 | 1.32 ± 0.06 | 4.98 ± 0.23 | 3.8 ± 0.2 |
| VI179 | 1.69 ± 0.07 | 8.30 ± 0.33 | 4.9 ± 0.3 |
| VI180 | 2.92 ± 0.20 | 114.75 ± 4.44 | 39.3 ± 3.1 |
| VI182 | 3.21 ± 0.16 | 61.61 ± 3.64 | 19.2 ± 1.5 |
| VI184 | 2.15 ± 0.11 | 109.28 ± 5.43 | 50.8 ± 3.6 |
| VI185 | 1.59 ± 0.10 | 7.07 ± 0.31 | 4.4 ± 0.3 |
| VI186 | 1.67 ± 0.12 | 143.87 ± 9.25 | 86.1 ± 8.3 |

^a The excision frequency was quantified by measuring the percentage of cells with unoccupied *attB* sites by real-time quantitative PCR. The values presented are the means and standard deviations of the results from triplicate measurements.

^b The ratio was calculated as percentage of *attP*/percentage of *attB*. In the ideal case of a strain harboring a single SXT, the expected value of this ratio is 1, since the excision of a single SXT theoretically generates an *attB* site and an *attP* site per chromosome.

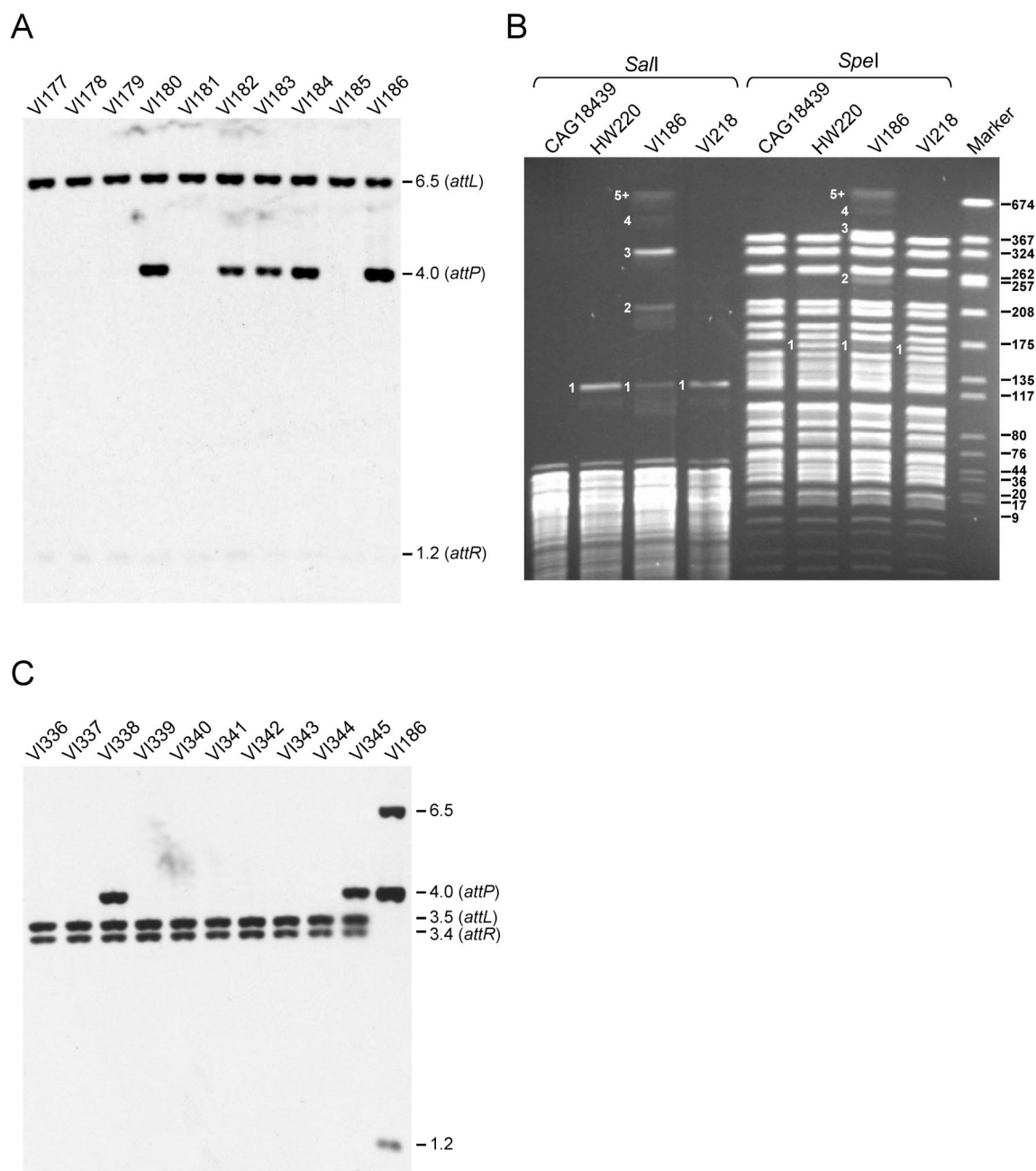


FIG. 1. Tandem arrays of SXTs. (A) Southern blot analysis of five pairs of *Tet*^r *Sxt*^r exconjugants resulting from five independent mating experiments between *E. coli* MG1655 *prfC*::SXT and *E. coli* CAG18439. The donor and recipient strains were mated for 6 h at 37°C on LB agar medium without selection. The purified total genomic DNAs of the *Tet*^r *Sxt*^r exconjugants were digested with *EcoRI*/*EcoRV* and analyzed by Southern blot hybridization with the 600-bp *Bst*BI fragment of pVI8A containing *attP* from SXT as a probe. The molecular sizes in kilobases correspond to the fragments containing the *attL* (6.5 kb, *EcoRV*), *attP* (4.0 kb, *EcoRI*/*EcoRV*), and *attR* (1.2 kb, *EcoRI*/*EcoRV*) junction fragments. (B) Contour-clamped homogenous PFGE of *SalI* or *SpeI* restriction patterns of *E. coli* CAG18439 (*Sxt*^r), HW220 (*Sxt*^r), VI186 (*Sxt*^r), and VI218 (*Sxt*^r). The gel electrophoresis was carried out for 30 h at 5 V/cm. The size marker (Marker) was *SmaI*-digested chromosomal DNA of *Staphylococcus aureus* NCTC8325. The molecular sizes indicated to the right of the panel are in kilobases. The numbers indicated to the left of the bands on the HW220, VI186, and VI218 restriction patterns correspond to the copy numbers of SXT in each fragment. The size of the fragments 1 to 5+ observed in the VI186 restriction pattern are, respectively, 125, 224.5, 324, 424.4, and 522.9 kb or more for *SalI*, and 165.9, 265.4, 364.8, 464.3, and 563.8 kb or more for *SpeI*. (C) Southern blot analysis of 10 *Kan*^r *Sxt*^r exconjugants (VI336 to VI345) resulting from a mating between *V. cholerae* MO10 and *V. cholerae* E4. *E. coli* VI186 was used as a control. The fragments containing the *V. cholerae attL* and *attR* are shown.

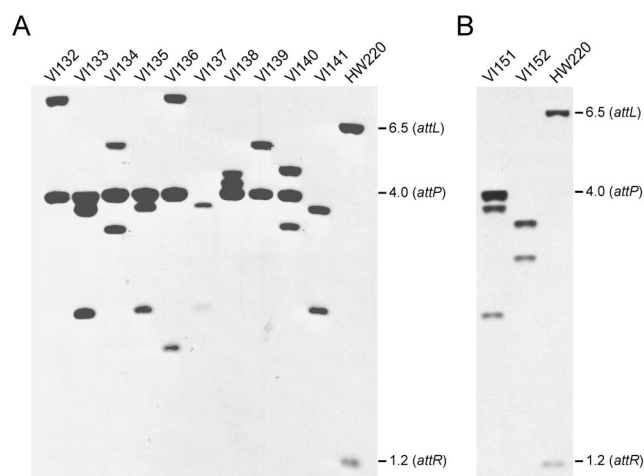


FIG. 2. Tandem arrays in *recA* and Δ *prfC* mutant strains of *E. coli*. Southern blot analyses of Tet⁺ Sxt⁺ exconjugants resulting from mating experiments involving a *recA*⁺ Δ *prfC* strain (VI131) (A) or a *recA* Δ *prfC* strain (VI147) (B) as the recipient. *E. coli* VI166 (BW25113 *prfC*::SXT) was used as a donor strain in both experiments. The donor and recipient strains were mated for 6 h at 37°C on LB agar medium without selection. The purified total genomic DNAs of the Tet⁺ Sxt⁺ exconjugants were digested with EcoRI/EcoRV and analyzed by Southern blot hybridization with the 600-bp BstBI fragment of pV18A containing *attP* from SXT as a probe. The molecular sizes in kilobases correspond to the fragments containing the *attL* (6.5 kb, EcoRV), *attP* (4.0 kb, EcoRI/EcoRV), and *attR* (1.2 kb, EcoRI/EcoRV) junction fragments in *E. coli* HW220 (CAG18439 *prfC*::SXT) used as a control strain.

presence of antibiotic selection. Growth of HW220 in LB broth containing various concentrations of sulfamethoxazole (from 160 μ g/ml to 2.5 mg/ml) and trimethoprim (from 32 μ g/ml to 512 μ g/ml) did not promote SXT amplification as measured by *attP* quantification by real-time quantitative PCR (data not shown).

Formation of SXT arrays does not require *recA* or *prfC*. Several mechanisms could account for the formation of tandem SXT arrays. Serial SXT transfer from multiple donor cells (or even a single donor cell) to a single recipient strain could lead to the formation of arrays by *recA*-dependent recombination between an incoming element and an already integrated SXT. To assess the role of homologous recombination in the formation of tandem SXT arrays, the *E. coli* *recA* mutant strain KB1 was used as a recipient in mating experiments with the *recA*⁺ donor strain VI166. Quantification of *attP* percentages in exconjugants revealed that 2 of 10 exconjugants tested carried tandem SXT arrays (data not shown), indicating that *recA* is not required for the formation of SXT arrays.

We previously found that *prfC*, the SXT primary integration site, was not absolutely required for SXT integration and that SXT can integrate into alternative sites (7). We excluded the possibility that the SXT integration site within *prfC* was required for SXT array formation by using VI131, a Δ *prfC* derivative of *E. coli* MG1655 as a recipient (Table 1). Eight of ten exconjugants derived from a mating of VI166 and VI131 harbored SXT tandem arrays. This was seen as the amplified *attP*-containing fragment in Southern blot analysis of DNA from these exconjugants (Fig. 2A). Similarly, when VI147, a *recA* Δ *prfC* mutant, was used as a recipient, an amplified *attP*-

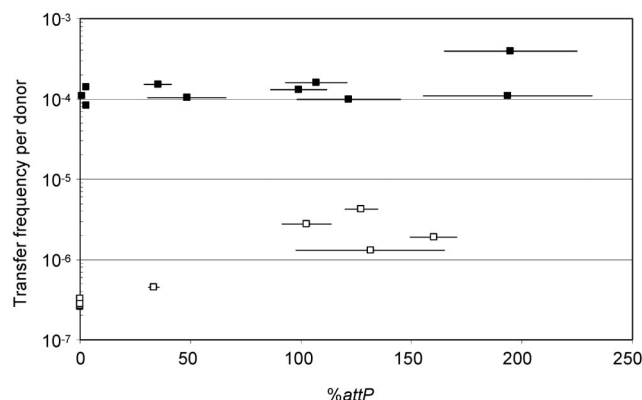


FIG. 3. Effect of the tandem arrays on the transfer frequency of SXT Δ *xis*. The frequencies of exconjugant formation per donor were obtained by dividing the number of exconjugants (Nal^r Sxt⁺ CFU) by the number of donor cells (Tc^r CFU). In all of the mating experiments, the recipient strain was *E. coli* B1533 (MG1655 Nal^r). The donors were *E. coli* exconjugants obtained from mating VI200 (MG1655 *prfC*::SXT Δ *xis* pXis) \times CAG18439 (\square) or from mating VI166 (BW25113 *prfC*::SXT) \times CAG18439 (\blacksquare). The expression of *xis* by pXis in the donor strain VI200 was induced with 0.02% arabinose during the mating experiments on LB agar plates. Real-time quantitative PCR was used to determine the percentage of *attP* sequences resulting from SXT excision and tandem SXT array formation. Triplicate measurements were performed on each sample, and the means and standard deviations (horizontal bars) are presented for each assay. DNA templates were prepared from overnight LB broth cultures.

containing fragment was detected in 1 of 2 exconjugants tested (Fig. 2B). Together, these data indicate that neither the SXT primary integration site *prfC* nor homologous recombination is required in the formation of tandem SXT arrays. Instead, we hypothesize that multiple integrations of circular SXTs occur by Int-mediated site-specific recombination into the *attL* or *attR* of an already integrated SXT.

Tandem structures increase the transfer efficiency of a Δ *xis* SXT mutant. To investigate the effect of tandem SXT arrays on the frequency of exconjugant formation, we isolated 10 randomly selected fresh Sxt⁺ exconjugants derived from a mating where the donor strain harbored a single copy of SXT. These exconjugants were then used as donors in new mating assays, and the percentage of *attP* was measured for each of these donors. As shown in Fig. 3, there was no significant correlation between the frequency of SXT transfer and the percentage of *attP* in the exconjugants used as donors.

Our previous work suggested that, with a Δ *xis* SXT donor, the formation of the extrachromosomal form of SXT was a key step in limiting SXT transfer, since the Δ *xis* SXT cells were 3 orders of magnitude less efficient as donors than cells harboring a single copy of wild-type SXT (7). We wondered whether tandemly arranged Δ *xis* SXTs could at least partially complement the transfer deficiency of a single Δ *xis* SXT donor. An experiment similar to the one described above was carried out to explore this possibility. An initial donor strain harboring a single Δ *xis* SXT in which Xis was provided in *trans* was used to generate Δ *xis* SXT exconjugants. These exconjugants were then used as donors. The frequency of exconjugant formation from these new donors varied between 2.6×10^{-7} and $4.2 \times$

10^{-6} exconjugants/donor (a 16-fold variation). There was a general correlation between the percentage of *attP* in the donor strain and the frequency of exconjugant formation (Fig. 3). The percentage of *attP* in 5 of the 10 donors was nearly undetectable (Fig. 3), and these strains were extremely inefficient donors. These strains likely contained a single Δxis SXT, given the very low excision frequency previously observed for the single Δxis SXT (7). The percentage of *attP* for the five other donors was significantly higher, and these strains were more efficient donors (Fig. 3). The overall trend of the data presented in Fig. 3 shows that tandem Δxis SXT arrays can, at least in part, rescue the transfer deficiency of Δxis SXT mutants. This result could be meaningful in hosts in which SXT is unable to excise.

Tandem SXT and R391 form hybrid elements. It is not clear how strains harboring Δxis SXT generate extrachromosomal circular SXT DNA or why transfer was higher from strains carrying tandem Δxis SXT arrays. One possibility to explain the latter observation is that the production of Int, required for excision, is higher in cells harboring tandem arrays; however, we previously showed that Int overexpression does not increase the frequency of excision and transfer (7). Another possibility is that tandem arrays allow for different processes for production of the extrachromosomal SXT DNA required for its transfer. For example, extrachromosomal SXT might arise through homologous recombination between adjacent integrated elements. Alternatively, a replicative process, analogous to that used by tandemly arranged CTX prophages (19) might generate extrachromosomal SXT DNA. Both of these processes are expected to yield hybrids containing sequences from adjacent elements. To explore whether either of these models could explain how extrachromosomal SXT DNA is generated by Δxis ICE arrays, we tested whether hybrid ICEs would indeed form by using tandem arrays of SXT and R391 (Kan^r Mer^r). The structure of the hybrids would vary for the two models. If replication initiating at the 5' *oriT* and extending to the 3' *oriT* in a tandem array generates the extrachromosomal DNA, only one hybrid element would arise from donor cells containing Δxis SXT- Δxis R391 arrays (Fig. 4A). Alternatively, if transfer from *xis*-deleted arrays depends upon homologous recombination, then many different hybrid elements would arise from donor cells containing Δxis SXT- Δxis R391 arrays, since these ICEs share large segments of identical DNA.

For these experiments, the *recA*⁺ strains JO115 and JO116 (Table 1), which harbor tandem arrays of wild-type R391-SXT and SXT-R391, respectively (14), were used as donors. We analyzed Sxt^r Kan^s exconjugants when JO115 was used as a donor and Sxt^s Kan^r exconjugants when JO116 was used as a donor because these exconjugants would be more likely to include hybrids that arise from either the replication-based or homologous recombination-based mechanisms outlined above. The structure of exconjugants was analyzed using PCR assays that detect SXT- or R391-specific sequences (Fig. 4B and C). Hybrid elements were readily found. One of the two Sxt^r Kan^s exconjugants harbored a recombinant ICE, AD1, containing the left part of SXT including *s037* but not *s052* and the right part of R391 (Fig. 4D). One of the six Sxt^s Kan^r exconjugants harbored a recombinant element, CB1, that contained most of R391 and a small region from the right part of SXT. Therefore, donors like JO115 and JO116, where each ICE can excise and

transfer independently, can also give rise to hybrid ICEs. While the hybrid AD1 could have arisen from the *oriT*-to-*oriT* replication-based mechanism of generation of extrachromosomal DNA, the hybrid ICE CB1 cannot be explained by such a mechanism because it does not include *s052*, a gene that lies 3' of the SXT *oriT* (Fig. 4A and D). Both AD1 and CB1 were functional ICEs and transferred with frequencies similar to that of R391 (Table 4). The process of conjugative transfer appears to be required for generation of recombinant elements from the tandem arrays in JO115 and JO116. We were unable to detect formation of hybrid elements in either of these two strains when they were cultured in the absence of a recipient (data not shown).

Next, we evaluated the role of homologous recombination in transfer from tandem arrays of Δxis elements. We constructed a Δxis R391- Δxis SXT array and a Δxis SXT- Δxis R391 array in a *recA* *E. coli* strain, yielding VI227 and VI228, respectively (Table 1). We produced SetC and SetD from a plasmid in these strains to bypass RecA's role as a regulator for transfer gene expression. Surprisingly, these two strains were extremely efficient donors. The frequency of transfer of each marker to a *recA*⁺ recipient, *E. coli* BI533, was even higher than that observed with *xis*⁺ donors (Table 5). Transfer from these *recA* donors indicates that homologous recombination is not required for formation of extrachromosomal ICE DNA in Δxis donors containing R391-SXT arrays.

Some of the exconjugants derived from both VI227 and VI228 donors contained hybrid elements composed of parts from SXT and R391. For example, two of the Kan^s Sxt^r exconjugants derived from the VI227 donor were found to carry recombinant elements, AD2 and CB2. AD2 contained the left part of SXT and the right part of R391 and CB2 contained the left part of R391 and the right part of SXT (Fig. 4D). Since the hybrids AD2 and CB2 arose from the same donor, the relative position of SXT and R391 in the tandem arrays does not appear to determine the structure of the resulting hybrid element. Two of the Kan^r Sxt^s exconjugants derived from the VI228 donor harbored hybrids, CB3 and CB4, that possessed the left part of R391 and the right part of SXT, although these hybrid ICEs were not identical (Fig. 4D). The identification of hybrids arising from *recA* donors ruled out the involvement of homologous recombination in the donor. Furthermore, the variety of hybrids detected is additional evidence that a replicative process initiating at the 5' *oriT* in a Δxis SXT- Δxis R391 array cannot be the sole explanation for transfer from such arrays nor for the generation of hybrid elements. All of the hybrid ICEs tested were capable of transfer to new hosts (Table 4).

We performed similar experiments with the same donor strains but with a *recA* *E. coli* recipient to verify that homologous recombination did not take place in recipient cells. The transfer frequencies of both markers were comparable to those observed in the experiments involving the *recA*⁺ recipient (Table 5). We isolated two distinct hybrid elements, CB5 and CB6, from 48 randomly selected Sxt^s Kan^r exconjugants. CB5 was derived from the VI227 donor, and CB6 was derived from the VI228 donor (Fig. 4D). Thus, homologous recombination in recipient cells is not required in the formation of hybrid ICEs.

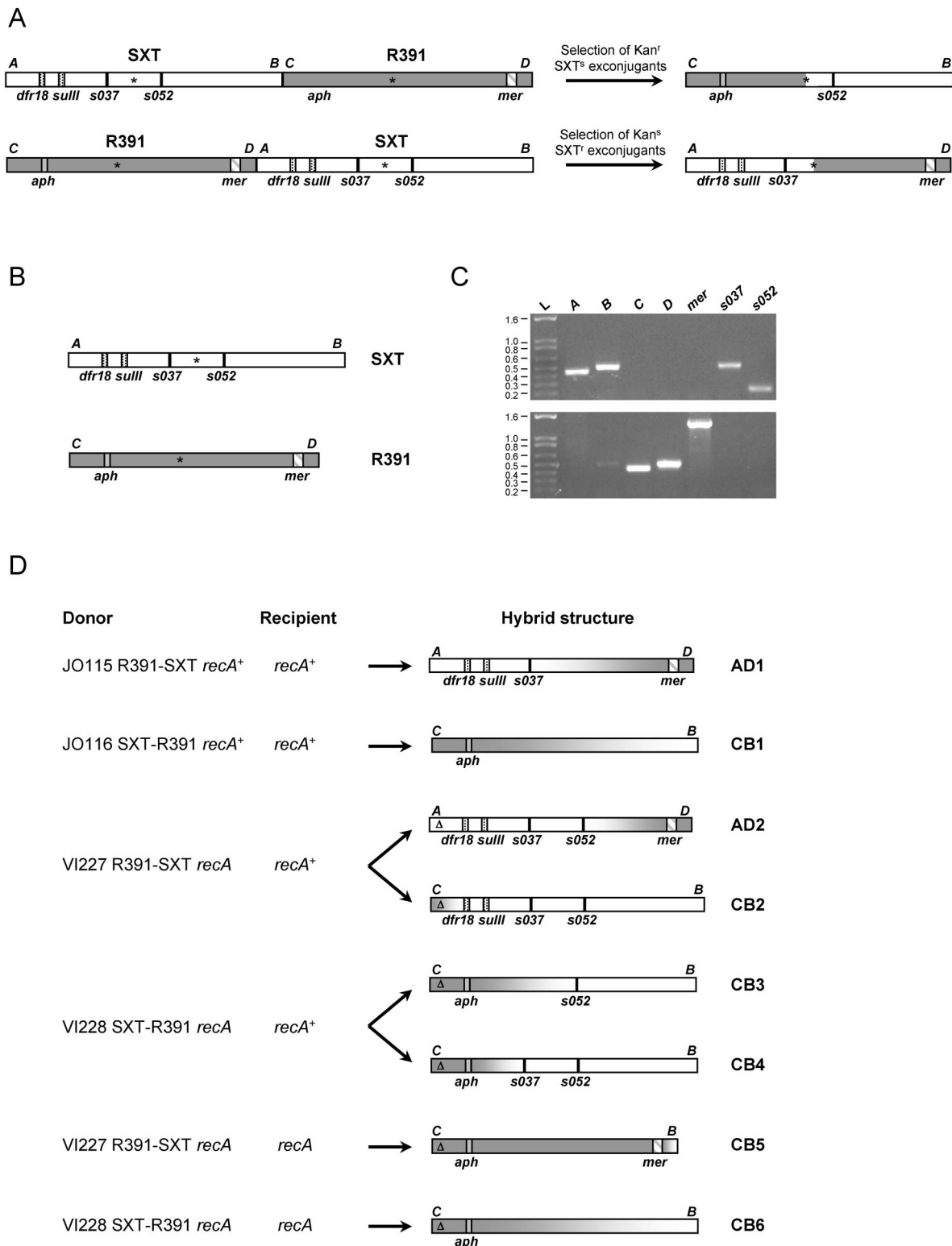


FIG. 4. Analysis of hybrids formed by recombination between SXT and R391. (A) Schematic representation of the structures of the tandem arrays SXT-R391 and R391-SXT and predicted hybrid ICEs formed by the *oriT*-to-*oriT* replication-based mechanism. (B) Schematic representation of the structures of SXT and R391. *mer*, *aph*, *sulII*, and *dfr18* encode, respectively, resistances to mercury, kanamycin, sulfamethoxazole, and trimethoprim. The asterisks indicate the positions of the *oriT* in SXT and the probable *oriT* in R391. (C) Amplification of sequences specific to SXT and R391. The fragments A (452 bp) and C (449 bp) are specifically amplified from the left part of SXT and R391, respectively, with the primer sets VISLF-VISLR3 and VISLF-VISLR2 (Table 2). The fragments B (509 bp) and D (511 bp) are specifically amplified from the right part of SXT and R391, respectively, with the primer sets VISRF-VIRR and VISRF-VISRR2. *mer* is a 1,371-bp fragment amplified from R391 with

TABLE 4. Mobility properties of hybrid elements

| Element ^a | Transfer frequency (10 ⁻⁴) ^b | Excision frequency (%) ^c | |
|----------------------|---|-------------------------------------|-------------|
| | | <i>attB</i> | <i>attP</i> |
| Δ <i>xis</i> SXT | 0.26 | 2.6 ± 0.2 | 3.9 ± 0.4 |
| Δ <i>xis</i> R391 | 2.4 | 3.2 ± 0.6 | 2.0 ± 0.4 |
| AD1 | 2.1 | 7.8 ± 1.3 | 18.6 ± 2.7 |
| CB1 | 5.6 | 1.5 ± 0.2 | 3.5 ± 0.5 |
| AD2 | 0.035 | 5.5 ± 2.6 | 11.4 ± 4.5 |
| CB2 | 2.1 | 3.2 ± 0.6 | 2.9 ± 0.6 |
| CB3 | 4.1 | 5.1 ± 1.2 | 4.5 ± 0.9 |
| CB4 | 3.9 | 6.7 ± 0.6 | 5.2 ± 0.9 |

^a In the donor strains harboring Δ*xis* SXT, Δ*xis* R391, AD2 CB2, CB3, and CB4, *Xis* was provided by p*Xis*, expressing *xis* under control of P_{BAD} to complement the Δ*xis* mutation of the elements.

^b Transfer frequency was calculated as the frequency of exconjugants per recipient and is the mean value of the results from three independent experiments. The selected markers were *aph* (Kan^r) for R391, CB1, CB3, and CB4 or *dfr18* and *sulII* (Sxt^r) for SXT, AD1, AD2, and CB2.

^c The excision frequency was quantified by measuring the percentage of unoccupied *attB* sites and the percentage of *attP* sites by real-time quantitative PCR. The values are the means and standard deviations of the results from three independent measurements.

DISCUSSION

Tandem arrays of SXT were frequently found in freshly derived SXT exconjugants. There was considerable heterogeneity in the size of SXT arrays present in cells from a single colony. Some of these arrays contained more than five copies, indicating that SXT arrays could represent greater than 10% of the *E. coli* genome. However, these large arrays were unstable and did not persist through serial passage. The mechanism that underlies the formation of SXT arrays is not known, but array formation appears to depend upon conjugative transfer of SXT, since we did not detect arrays following serial passage of a strain harboring a single SXT. Besides illustrating the dynamic nature of chromosome structure in SXT exconjugants, formation of SXT arrays has functional consequences. The presence of SXT arrays can partially rescue the defect in SXT transfer that occurs in the absence of *Xis*. Furthermore, SXT-R391 arrays facilitate the emergence and evolution of novel ICEs by enabling formation of hybrid elements.

The heterogeneity in SXT copy number in fresh exconjugants was observed in quantitative PCR assays and Southern blots measuring the amount of *attP* in exconjugants as well as in PFGE analyses. The percentages of *attP* sites in exconjugants were never integer multiples of 100%, as expected for discrete SXT copy numbers. The fact that we did not detect such values reflects the variation in the sizes of the SXT arrays among cells from individual exconjugant colonies. The *attP* percentage measured by this PCR assay represents the mean value of the SXT copy number. Thus, even if strains have similar *attP* percentages, the distribution of SXT copy number

TABLE 5. Frequency of transfer of the kanamycin and SXT markers

| Donor | Relevant genotype ^a | Recipient | Relevant genotype | Transfer frequency (10 ⁻³) ^b with selection for: | |
|-------|-----------------------------------|-----------|--------------------------|---|------|
| | | | | Kanamycin | SXT |
| JO115 | R391-SXT <i>recA</i> ⁺ | BI533 | <i>recA</i> ⁺ | 0.43 | 0.18 |
| JO116 | SXT-R391 <i>recA</i> ⁺ | BI533 | <i>recA</i> ⁺ | 0.45 | 0.21 |
| VI227 | R391Δ-SXTΔ <i>recA</i> | BI533 | <i>recA</i> ⁺ | 20.4 | 4.7 |
| VI228 | SXTΔ-R391Δ <i>recA</i> | BI533 | <i>recA</i> ⁺ | 107.6 | 1.8 |
| VI227 | R391Δ-SXTΔ <i>recA</i> | MW5-39 | <i>recA</i> | 10.0 | 5.5 |
| VI228 | SXTΔ-R391Δ <i>recA</i> | MW5-39 | <i>recA</i> | 70.4 | 0.5 |

^a Δ indicates the deletion of *xis*. The *recA* donors carried pSetCD to provide SetC and SetD, which activate the expression of the transfer genes.

^b The frequency of transfer was calculated by determining the number of exconjugants per recipient, since the overexpression of *setC* and *setD* in presence of SXT is detrimental to the growth of the donor cells. The transfer frequencies are the means of the results from three independent experiments. The mating experiments were carried out for 6 h at 37°C, and the medium was supplemented with 0.02% arabinose when the donors carried pSetCD.

in the cell populations may vary. Although an idea about the distribution of SXT copy number cannot be gleaned from the quantitative PCR analyses, the PFGE analysis, as shown in Fig. 1B, provides information regarding this distribution.

We found that the percentage of unoccupied *attB* sites remains relatively constant, varying from 1.32 to 3.21%, irrespective of the percentage of *attP* sites (i.e., of the presence or size of SXT arrays) in a strain. The relative stability of the excision frequency may indicate that entire SXT arrays excise as a single circular molecule by recombination between the most distal *attL* and *attR* sites flanking the array. Recombination involving internal *attP* sites between adjacent SXTs in an array could be inhibited due to interactions with *Xis*, since this protein apparently inhibits recombination between *attP* and *attB*, preventing SXT integration (7).

Although formation of tandem SXT arrays appears to occur frequently in exconjugants from both *E. coli* and *V. cholerae*, these arrays were transient. Preliminary observations suggest that tandem SXT arrays are stable in the absence of *recA* (data not shown). Homologous recombination between the elements in a tandem array may lead to reductions in array size. We were unable to find SXT tandem arrays in *V. cholerae* Sxt^r clinical isolates (data not shown), suggesting that arrays are also unstable in natural isolates.

SXT is not the only ICE to form tandem arrays, R391 arrays were also found in freshly derived exconjugants (data not shown). Furthermore, tandem arrays of the 105-kb *clc* element, an ICE derived from *Pseudomonas* sp. strain B13, which contains genes for chlorocatechol degradation, have been reported previously (20). Interestingly, Ravatn et al. reported a correlation between the *clc* copy number in exconjugants and their

MER104A and MER103B. It covers the middle of the *mer* operon of R391. The fragments *s037* (523 bp) and *s052* (242 bp) are specific to SXT and were amplified with the primer sets 10SF13-SXT1-13 and YND2-ORF16, respectively. The sizes of the ladder (L) are given in kilobases. (D) Schematic representation of the structures of the isolated hybrid ICEs. The structure of the hybrids was deduced from the antibiotic resistance phenotype and from the pattern of SXT- and R391-specific fragments detected by PCR, as shown in panel A. The positions of the amplified fragments and the genes encoding the antibiotic resistance are indicated. The precise position of the point of recombination in each hybrid is not known, but it is deduced from the presence or absence of the markers tested. The gradient from white to dark gray indicates the fragment within which the recombination probably took place to generate the hybrids. Δ, Δ*xis* mutation.

capability to grow on chlorobenzene as the sole carbon source and suggested that the selective pressure exerted by the substrate influenced the *clc* copy number (20). In contrast, our work suggests that tandem arrays of SXT or R391 arise as a consequence of the conjugative process itself, since we were unable to detect SXT arrays in a strain that initially contained a single copy of SXT, even on sulfamethoxazole and trimethoprim-supplemented medium.

Several conjugation-dependent mechanisms could explain the formation of SXT arrays. Tandem arrays could form after transfer of several copies of the element from a single donor cell to a single recipient cell. This could occur if a concatemer of several copies of SXT was transferred to a recipient. Alternatively, a single donor may transfer several copies of single SXT to the same recipient. The formation of SXT arrays could also occur following transfer of a single SXT from several donors to a single recipient cell. Given the homology of SXT transfer-related genes to those of conjugative plasmids, we assume that a single-stranded SXT, generated by a rolling-circle-like process, is transferred from donor to recipient.

It was previously shown that SXT and R391 are able to use an *attL* or *attR* site for integration (14). Since we found that *recA* was not required for the formation of SXT arrays, if multiple transfers of SXT account for the generation of the arrays, SXT integration into the recipient chromosome probably occurs by an Int-mediated site-specific recombination event into the *attL* or *attR* site of a previously integrated element. We found that *prfC*, the SXT primary integration site, is not required for the formation of SXT arrays. Therefore, if multiple rounds of SXT transfer occur in a $\Delta prfC$ mutant already containing an SXT, the novel *attL* or *attR* sites are sufficient for SXT integration. Given the relatively low frequency of transfer of SXT and R391, it seems improbable that multiple donors transfer SXT to the same recipient. However, it is possible that there is some period of time after a recipient has acquired SXT, during which it is transiently highly proficient as a donor. When SXT has just entered a new host cell, the level of the repressor SetR may not be sufficient to repress expression of the *tra* genes. Epidemic spread of F-like conjugative plasmids from recent exconjugants has been reported (30). Perhaps SXT arrays form after a burst of SXT transfer from recent recipients to new recipients and to former donors.

Tandem SXT-R391 arrays in donor cells can lead to the formation of hybrid ICEs in exconjugants. Each hybrid ICE we identified was able to excise and transfer by conjugation to new recipients. Some of these hybrids, like AD1 and AD2, confer resistance to SXT and likely to mercury as well, two phenotypes specific to each parental element. Therefore, heterogeneous tandem ICE arrays facilitate the generation of ICEs with novel combinations of properties and contribute to the plasticity of this family of elements. Although the mechanism generating these hybrid elements is still unknown, we showed that neither homologous recombination nor *oriT*-to-*oriT* replication is required in their formation. Since SXT and R391 both contain orthologues of the Bet recombination protein found in several bacteriophages (54% identity of SXT S065 and R391 Orf68 with Bet protein of phage λ) (2, 4), we hypothesize that these recombinases play a role in the formation of the hybrid ICEs.

ACKNOWLEDGMENTS

We thank B. Davis, A. Kane, S. McLeod, and J. Ritchie for critical reading of the manuscript. We are grateful to L. McDermott for help with the PFGE experiments.

This work was supported by funds from NIH grant AI42347, the Howard Hughes Medical Institute, and the NEMC GRASP Center (grant P30DK-34928).

REFERENCES

1. Beaber, J. W., V. Burrus, B. Hochhut, and M. K. Waldor. 2002. Comparison of SXT and R391, two conjugative integrating elements: definition of a genetic backbone for the mobilization of resistance determinants. *Cell. Mol. Life Sci.* **59**:2065–2070.
2. Beaber, J. W., B. Hochhut, and M. K. Waldor. 2002. Genomic and functional analyses of SXT, an integrating antibiotic resistance gene transfer element derived from *Vibrio cholerae*. *J. Bacteriol.* **184**:4259–4269.
3. Beaber, J. W., B. Hochhut, and M. K. Waldor. 2004. SOS response promotes horizontal dissemination of antibiotic resistance genes. *Nature* **427**:72–74.
4. Boltner, D., C. MacMahon, J. T. Pembroke, P. Strike, and A. M. Osborn. 2002. R391: a conjugative integrating mosaic comprised of phage, plasmid, and transposon elements. *J. Bacteriol.* **184**:5158–5169.
5. Burrus, V., G. Pavlovic, B. Decaris, and G. Guedon. 2002. Conjugative transposons: the tip of the iceberg. *Mol. Microbiol.* **46**:601–610.
6. Burrus, V., G. Pavlovic, B. Decaris, and G. Guedon. 2002. The ICES/I element of *Streptococcus thermophilus* belongs to a large family of integrative and conjugative elements that exchange modules and change their specificity of integration. *Plasmid* **48**:77–97.
7. Burrus, V., and M. K. Waldor. 2003. Control of SXT integration and excision. *J. Bacteriol.* **185**:5045–5054.
8. Chu, G., D. Vollrath, and R. W. Davis. 1986. Separation of large DNA molecules by contour-clamped homogeneous electric fields. *Science* **234**:1582–1585.
9. Coetzee, J. N., N. Datta, and R. W. Hedges. 1972. R factors from *Proteus rettgeri*. *J. Gen. Microbiol.* **72**:543–552.
10. Dalsgaard, A., A. Forslund, D. Sandvang, L. Arntzen, and K. Keddy. 2001. *Vibrio cholerae* O1 outbreak isolates in Mozambique and South Africa in 1998 are multiple-drug resistant, contain the SXT element and the *aadA2* gene located on class 1 integrons. *J. Antimicrob. Chemother.* **48**:827–838.
11. Datsenko, K. A., and B. L. Wanner. 2000. One-step inactivation of chromosomal genes in *Escherichia coli* K-12 using PCR products. *Proc. Natl. Acad. Sci. USA* **97**:6640–6645.
12. Goldberg, L., and J. J. Mekalanos. 1986. Effect of a *recA* mutation on cholera toxin gene amplification and deletion events. *J. Bacteriol.* **165**:723–731.
13. Heath, J. D., J. D. Perkins, B. Sharma, and G. M. Weinstock. 1992. *NotI* genomic cleavage map of *Escherichia coli* K-12 strain MG1655. *J. Bacteriol.* **174**:558–567.
14. Hochhut, B., J. W. Beaber, R. Woodgate, and M. K. Waldor. 2001. Formation of chromosomal tandem arrays of the SXT element and R391, two conjugative chromosomally integrating elements that share an attachment site. *J. Bacteriol.* **183**:1124–1132.
15. Hochhut, B., Y. Lotfi, D. Mazel, S. M. Faruque, R. Woodgate, and M. K. Waldor. 2001. Molecular analysis of antibiotic resistance gene clusters in *Vibrio cholerae* O139 and O1 SXT constains. *Antimicrob. Agents Chemother.* **45**:2991–3000.
16. Hochhut, B., J. Marrero, and M. K. Waldor. 2000. Mobilization of plasmids and chromosomal DNA mediated by the SXT element, a constin found in *Vibrio cholerae* O139. *J. Bacteriol.* **182**:2043–2047.
17. Hochhut, B., and M. K. Waldor. 1999. Site-specific integration of the conjugal *Vibrio cholerae* SXT element into *prfC*. *Mol. Microbiol.* **32**:99–110.
18. Miller, J. H. 1992. A short course in bacterial genetics. Cold Spring Harbor Laboratory Press, Cold Spring Harbor, N.Y.
19. Moyer, K. E., H. H. Kimsey, and M. K. Waldor. 2001. Evidence for a rolling-circle mechanism of phage DNA synthesis from both replicative and integrated forms of CTX ϕ . *Mol. Microbiol.* **41**:311–323.
20. Ravatn, R., S. Studer, D. Springael, A. J. Zehnder, and J. R. van der Meer. 1998. Chromosomal integration, tandem amplification, and deamplification in *Pseudomonas putida* F1 of a 105-kilobase genetic element containing the chlorocatechol degradative genes from *Pseudomonas* sp. strain B13. *J. Bacteriol.* **180**:4360–4369.
21. Rice, L. B. 1998. Tn916 family conjugative transposons and dissemination of antimicrobial resistance determinants. *Antimicrob. Agents Chemother.* **42**:1871–1877.
22. Sambrook, J., E. F. Fritsch, and T. Maniatis. 1989. Molecular cloning: a laboratory manual, 2nd ed. Cold Spring Harbor Laboratory, Cold Spring Harbor, N.Y.
23. Singer, M., T. A. Baker, G. Schnitzler, S. M. Deischel, M. Goel, W. Dove, K. J. Jaacks, A. D. Grossman, J. W. Erickson, and C. A. Gross. 1989. A collection of strains containing genetically linked alternating antibiotic resistance elements for genetic mapping of *Escherichia coli*. *Microbiol. Rev.* **53**:1–24.

24. **Sullivan, J. T., and C. W. Ronson.** 1998. Evolution of rhizobia by acquisition of a 500-kb symbiosis island that integrates into a phe-tRNA gene. *Proc. Natl. Acad. Sci. USA* **95**:5145–5149.
25. **Thungapathra, M., Amita, K. K. Sinha, S. R. Chaudhuri, P. Garg, T. Ramamurthy, G. B. Nair, and A. Ghosh.** 2002. Occurrence of antibiotic resistance gene cassettes *aac(6')-Ib*, *dfrA5*, *dfrA12*, and *ereA2* in class I integrons in non-O1, non-O139 *Vibrio cholerae* strains in India. *Antimicrob. Agents Chemother.* **46**:2948–2955.
26. **van der Meer, J. R., and V. Sentchilo.** 2003. Genomic islands and the evolution of catabolic pathways in bacteria. *Curr. Opin. Biotechnol.* **14**:248–254.
27. **Waldor, M. K., and J. J. Mekalanos.** 1994. ToxR regulates virulence gene expression in non-O1 strains of *Vibrio cholerae* that cause epidemic cholera. *Infect. Immun.* **62**:72–78.
28. **Waldor, M. K., H. Tschape, and J. J. Mekalanos.** 1996. A new type of conjugative transposon encodes resistance to sulfamethoxazole, trimethoprim, and streptomycin in *Vibrio cholerae* O139. *J. Bacteriol.* **178**:4157–4165.
29. **Whittle, G., N. B. Shoemaker, and A. A. Salyers.** 2002. The role of *Bacteroides* conjugative transposons in the dissemination of antibiotic resistance genes. *Cell. Mol. Life Sci.* **59**:2044–2054.
30. **Zatyka, M., and C. M. Thomas.** 1998. Control of genes for conjugative transfer of plasmids and other mobile elements. *FEMS Microbiol. Rev.* **21**:291–319.